

SIDDHARTA impact on $\bar{K}N$ amplitudes used in in-medium applications

A. Cieplý^{1,a} and J. Smejkal²

¹ Nuclear Physics Institute, 250 68 Řež, Czech Republic

² Institute of Experimental and Applied Physics, Czech Technical University in Prague, Horská 3a/22, 128 00 Praha 2, Czech Republic

Abstract. We have performed new fits of our chirally motivated coupled-channels model for meson–baryon interactions and discussed the impact of the SIDDHARTA measurement on the $\bar{K}N$ amplitudes in the free space and in nuclear medium. The kaon–nucleon amplitudes generated by the model are fully consistent with our earlier studies that used the older kaonic hydrogen data by the DEAR collaboration. The subthreshold energy dependence of the in-medium $\bar{K}N$ amplitudes plays a crucial role in \bar{K} –nuclear applications.

The recent measurement of kaonic hydrogen characteristics (the $1s$ level energy shift and width due to strong interaction) by the SIDDHARTA collaboration [1] tightens the constraints put on the theoretical models used to describe the low energy $\bar{K}N$ interactions. Unlike the older DEAR data [2] the new SIDDHARTA measurement is also consistent with the K^-p scattering length determined from the scattering data [3]. In this short report we examine the impact of the SIDDHARTA measurement on the K^-p and K^-n elastic amplitudes in the free space and in nuclear medium. The energy dependence of the K^-p amplitudes was already discussed in [4] and here we extend the analysis by showing our results for the K^-n elastic scattering amplitudes as well.

The modern treatment of kaon interactions with nucleons at low energies is based on effective field theory, the chiral perturbation theory (χ PT), combined with coupled channels techniques used to deal with divergencies that thwart the convergence of the χ PT expansion. We employ a chirally motivated separable potential model [5], [4] that matches the effective meson–baryon potentials to the chiral meson–baryon amplitudes obtained up to the second order in the χ PT expansion in meson momenta and quark masses. The model parameters (chiral Lagrangian couplings, the low energy constants, and the inverse ranges that define the off-shell form factors) are standardly fitted to the K^-p low energy cross sections, to the K^-p threshold branching ratios and to the $1s$ level characteristics of kaonic hydrogen. Interestingly, the lowest order (LO) Tomozawa–Weinberg interaction alone is quite sufficient to provide a reasonable fit to the experimental data, though the next-to-leading order (NLO) is relevant to achieve their good reproduction. An important feature of the theory is an energy dependence of the chiral SU(3) couplings that bind the various meson–baryon channels. Specifically, the coupling of the $\pi\Sigma$ and $\bar{K}N$ channels plays a major role for the dynamics of both meson–baryon states. It leads to an appearance of two dynamically generated isoscalar resonances [6] that are assigned to the $\Lambda(1405)$ resonance observed in the $\pi\Sigma$ mass spectrum just below the $\bar{K}N$ threshold.

In Ref. [4] we discussed results obtained with three different models and showed that all of them reproduce well the available experimental data for low energy K^-p interactions and the $\pi\Sigma$ mass distribution in the $\Lambda(1405)$ region. The models are (see [4] for details):

- TW1 - only Tomozawa–Weinberg interaction considered, just two parameters (inverse range and meson decay constant, both of them common to all channels) fitted to the experimental data including the SIDDHARTA measurement

^a e-mail: cieply@ujf.cas.cz

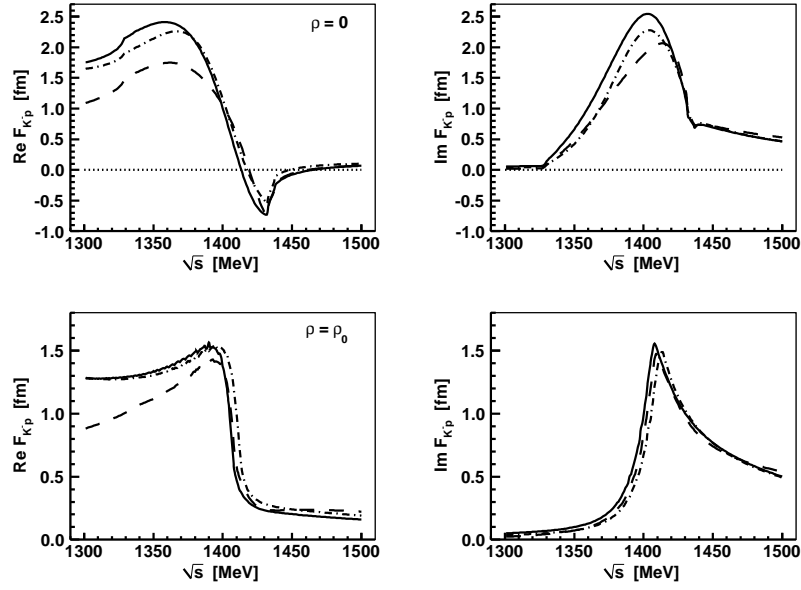


Fig. 1. Energy dependence of the real (left panels) and imaginary (right panels) parts of the elastic K^-p amplitude in the free space (top panels) and in the nuclear medium (bottom panels). Dashed curves: TW1 model, dot-dashed curves: CS30 model, solid curves: NLO30 model.

- NLO30 - all LO and NLO interaction terms considered, meson decay constants fixed on their physical values, three inverse ranges and four NLO d -couplings fitted to the experimental data including the SIDDHARTA measurement
- CS30 - an older LO+NLO model [5] whose parameters were fitted to the DEAR data instead of the new SIDDHARTA ones

The inclusion of the CS30 model allows us to compare the results obtained in the DEAR era with those refined due to the SIDDHARTA data. However, it was noted in Ref. [4] that the kaonic hydrogen characteristics computed with the CS30 model are already in a better agreement with the SIDDHARTA data rather than with the DEAR ones that were used in the fit. This fact underlines the much better consistency of SIDDHARTA with the other low energy data on K^-p scattering and reactions.

The energy dependence of the K^-N amplitudes in vacuum (nuclear density $\rho = 0$) and in nuclear medium ($\rho = \rho_0 = 0.17 \text{ fm}^{-3}$) is shown in figures 1 and 2. The quantity \sqrt{s} used for the x -axis represents the meson-baryon energy in the two-body CMS. The nuclear medium affects the $\bar{K}N$ interaction in two ways, due to Pauli blocking of the nucleons and due to selfenergies of the interacting particles. Both effects are included in our treatment of the in-medium amplitudes assuming a symmetric nuclear matter with proton and neutron densities $\rho_p = \rho_n = \rho_0/2$. It was demonstrated [7] that the two effects work partly against each other as the Pauli blocking pushes the $\Lambda(1405)$ resonance above the $\bar{K}N$ threshold and the meson and baryon selfenergies bring it back to energies about 30 MeV below the threshold. As a result the strong energy dependence of the K^-p amplitude is preserved in nuclear medium too.

The three models employed in our calculations lead to very similar K^-p amplitudes above the threshold and are in qualitative agreement at subthreshold energies as well. Interestingly, the Figure 1 also demonstrates that the NLO30 model fitted to the SIDDHARTA data [1] leads to K^-p amplitudes that are in close agreement with those obtained for the CS30 model fitted to the DEAR data [2]. Especially, the real parts of the amplitudes generated by the CS30 and NLO30 models are very close to each other when extrapolated as far as to (and even below) the $\pi\Sigma$ threshold. This feature may be explained by recalling that in fact the CS30 model was not able to reproduce the DEAR data and generates kaonic hydrogen characteristics that are more compatible with the SIDDHARTA results.

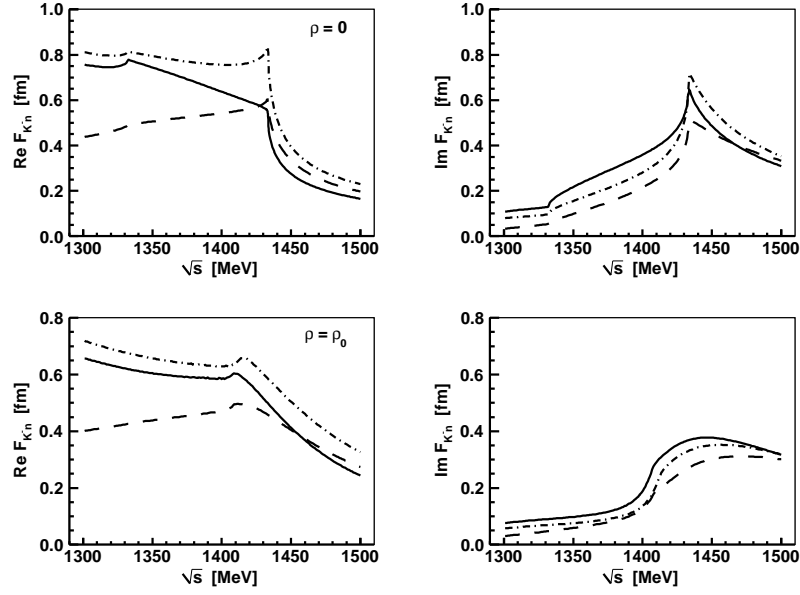


Fig. 2. Energy dependence of the real (left panels) and imaginary (right panels) parts of the elastic K^-n amplitude in the free space (top panels) and in the nuclear medium (bottom panels). Dashed curves: TW1 model, dot-dashed curves: CS30 model, solid curves: NLO30 model.

In other words, the energy dependence of the K^-p amplitude is to some extent fixed by the very precise threshold branching ratios and by the low energy scattering and reaction data (see Ref. [8] for a detailed analysis). The significance of the new SIDDHARTA data can be judged in terms of putting additional constraints on the models and reducing the theoretical uncertainties when extrapolating the K^-p interaction to subthreshold energies [9]. In nuclear medium, the qualitative behavior of the K^-p amplitude is once again independent of the model used in the calculations. It is remarkable that the selfconsistent treatment leads to even smaller differences between the CS30 and NLO30 models than they were in the free space, especially in the subthreshold energy region.

The K^-n elastic scattering amplitudes are shown in Fig. 2. The cusp structure observed for the free-space amplitude is related to the opening of the K^-n channel and to an existence of a pole in the scattering S -matrix, generated dynamically at the $[+,-]$ Riemann sheet (physical in the $\pi\Sigma$ channel and unphysical in the $\bar{K}N$ channel). Unlike for the K^-p amplitude the CS30 and NLO30 models lead to a different behavior of the real part of the K^-n amplitude in between the $\pi\Sigma$ and $\bar{K}N$ thresholds. This difference is caused partly by different positions of the isovector pole (with the pole generated for the CS30 model being closest to the physical region and to the K^-n threshold) and partly due to larger theoretical variations of the computed K^-n amplitude since the models are fixed solely to the K^-p data, not to the K^-n ones (since they are not any). In accordance with our observations for the K^-p system the nuclear medium effects (mainly the selfconsistent treatment of the kaon selfenergy) diminish the differences between the NLO30 and CS30 models. A shift of the cusp structure to lower energies is also consistent with our understanding of the in-medium dynamics. Finally, one should note the different scale of the y -axis in Figure 2 when compared with Figure 1. If the K^-n amplitude were plotted in the same scale as the K^-p one the energy dependence of the K^-n amplitude would appear much flatter, quite in line with the general consensus that the low energy $\bar{K}N$ interaction is governed by the isoscalar $\Lambda(1405)$ resonance and the energy dependence of the isovector $\bar{K}N$ amplitude is much weaker.

For a reference we also show in Table 1 the positions of the poles of the scattering S -matrix that govern the low energy K^-N interactions. The two isoscalar poles found on the second Riemann sheet $[-,+]$ are well known and assigned to the $\Lambda(1405)$ resonance. The existence of the isovector pole that

Table 1. The positions of the poles of the scattering S -matrix. The two isoscalar poles z_1 and z_2 are on the $[-,+]$ Riemann sheet (the signs relate to those of the imaginary parts of the meson–baryon CMS momenta in the channels $\pi\Sigma$ and $\bar{K}N$ in this order), the isovector pole z_3 resides on the $[+,-]$ Riemann sheet.

model	z_1 [MeV]	z_2 [MeV]	z_3 [MeV]
TW1	(1371 – i 54)	(1433 – i 25)	(1383 – i 53)
NLO30	(1355 – i 86)	(1418 – i 44)	(1410 – i 38)
CS30	(1398 – i 51)	(1441 – i 76)	(1416 – i 24)

relates to the structure observed in the K^-n amplitude is not so well documented. Though, it was already reported in Ref. [6], at the complex energy $z = (1401 - i 40)$ MeV. The Table 1 also illustrates how much model dependent are the exact positions of the poles.

The energy and density dependence of the K^-N amplitudes plays a key role in construction of the K^- –nuclear optical potential. Considering only one nucleon interactions we have

$$V_{\text{opt}}^K(\sqrt{s}, \rho) \sim F_{K^-p}(\sqrt{s}, \rho) \rho_p + F_{K^-n}(\sqrt{s}, \rho) \rho_n \quad .$$

It was demonstrated in Ref. [7] that the kaon–nucleon CMS energy \sqrt{s} is shifted to lower energies with respect to the kaon–nuclear CMS energy due to the binding of the hadrons in nuclear matter and due to their motion in the many body system. Thus, the K^- –nuclear interaction probes subthreshold $\bar{K}N$ energies where the K^-p in–medium amplitude exhibits much stronger attraction and the resulting K^- –nuclear optical potential becomes much deeper than when it were constructed from the amplitudes taken at the $\bar{K}N$ threshold. The energy shift to subthreshold energies provides a link between the shallow \bar{K} –nuclear potentials based on the chiral $\bar{K}N$ amplitudes evaluated at threshold and the deep phenomenological optical potentials obtained in fits to kaonic atoms data. The relevance of this finding to an analysis of kaonic atoms and quasi–bound \bar{K} –nuclear states was already investigated in Refs. [10] and [11].

We conclude that several versions of coupled–channels separable potential models considered in our work provide $\bar{K}N$ amplitudes that exhibit very similar energy dependence in the free space as well as in the nuclear medium. Specifically, the strong subthreshold energy and density dependence of the K^-p amplitudes, that reflects the dominant effect of the $\Lambda(1405)$ resonance, does not depend much on a particular version of the model. A prominent feature of the models is a sharp increase of K^-p in–medium attraction below the $\bar{K}N$ threshold that leads to much deeper \bar{K} –nuclear optical potentials than those that were derived from the amplitudes evaluated at the $\bar{K}N$ threshold.

Acknowledgement: The work was supported partly by the Grant Agency of Czech Republic, Grant No. P203/12/2126.

References

1. M. Bazzi *et al.* [SIDDHARTA Collaboration], Phys. Lett. B **704**, (2011) 113
2. G. Beer *et al.* [DEAR Collaboration], Phys. Rev. Lett. **94**, (2005) 212302
3. A. D. Martin, Nucl. Phys. B **179**, (1981) 33; and references therein
4. A. Cieplý, J. Smejkal, Nucl. Phys. A **881**, (2012) 115
5. A. Cieplý, J. Smejkal, Eur. Phys. J. A **43**, (2010) 191
6. D. Jido, J. A. Oller, E. Oset, A. Ramos, U.-G. Meißner, Nucl. Phys. A **725**, (2003) 181
7. A. Cieplý, E. Friedman, A. Gal, D. Gazda, J. Mareš, Phys. Rev. C **84**, (2011) 045206
8. B. Borasoy, U.-G. Meißner, R. Nißler, Phys. Rev. C **74**, (2006) 055201
9. Y. Ikeda, T. Hyodo, W. Weise, Nucl. Phys. A **881**, (2012) 98
10. E. Friedman, A. Gal, Nucl. Phys. A **881**, (2012) 150
11. D. Gazda, J. Mareš, Nucl. Phys. A **881**, (2012) 159